Premelting phenomena in ionic crystals

2008 J. Phys.: Condens. Matter 20 114116

(http://iopscience.iop.org/0953-8984/20/11/114116)

J. Phys.: Condens. Matter **20** (2008) 114116 (9pp) doi:10.1088/0953-8984/20/11/114116

Premelting phenomena in ionic crystals

Shigeki Matsunaga[1] **and Shigeru Tamaki**[2]

[1] Nagaoka National College of Technology, Nagaoka 940-8532, Japan
[2] Department of Physics, Faculty of Science, Niigata University, Japan

E-mail: matsu@nagaoka-ct.ac.jp,

Received 30 August 2007
Published 20 February 2008
Online at stacks.iop.org/JPhysCM/20/114116

Abstract
The theory of the premelting phenomena in ionic crystals has been developed on the basis of the concept of heterophase fluctuation in the vicinity of their melting points. The size of the liquid-like clusters is estimated by the theory using the experimental specific heat value. Molecular dynamics simulations are also performed in NaCl and AgBr crystals to examine the ionic configuration in the premelting region. The structural features are discussed using the Lindemann instability criterion.

(Some figures in this article are in colour only in the electronic version)

1. Introduction

In the higher temperature region, most ionic crystals have various relevant temperature dependences in their physical properties, such as ionic conductivity [1], specific heat [2], the thermal expansion coefficient [3], and so on [4]. Some of these in the vicinity of their melting points seem to be connected with the premelting phenomena [5].

Many years ago, Frenkel proposed a general theory of heterophase fluctuations in relation to the pre-transition phenomena including the premelting of solids [6]. The concept of Frenkel theory is that the liquid droplets occur in small regions of space and time of solids, which makes it possible to explain these anomalies satisfactorily. At the time of this proposal, unfortunately the experimental data were not sufficient, and there was a limitation to combining Frenkel theory and various experimental data. However, recent developments in the information from computer simulations and of various experimental data have caused us to re-evaluate Frenkel theory in order to estimate the size of small droplets proposed by Frenkel, by using some recent experimental data [2].

In section 2, we will discuss the origin of the heterophase fluctuation in the vicinity of the melting points of ionic crystals. In the following sections the Frenkel theory will be reconstructed, and furthermore we will derive several thermodynamic quantities due to such heterophase fluctuations in ionic crystals.

2. Fluctuation of defects in an ionic crystal

With increasing temperature in an ionic crystal, Schottky and/or Frenkel defects are produced in order to increase the entropy and eventually to diminish the total Gibbs free energy.

When the concentration of defects is relatively small, the distribution of defects seems to be random. On increasing the temperature, the increase of concentration naturally causes a defect–defect interaction. Using the Debye–Hückel approximation, Kurosawa obtained the result that the formation free energy of a pair of Schottky-type defects in an ionic crystal was lowered by the appearance of defect–defect interaction with increasing temperature [7]. According to him, the formation energy of a pair of Schottky-type defects E_V is expressed as follows:

$$E_V = -2k_B T \ln f - Af^{\gamma}, \tag{1}$$

where f is the fraction of defects to the total constituents. The last term of (1) is caused by the appearance of defect–defect interactions, in which A is a constant and γ is equal to $1/2$.

In the case of Frenkel-type defects, it is well known that the required energy to form an interstitial vacancy is a function of the available number of interstitial positions, and equation (1) is modified so as to satisfy such a condition.

Using the specific heat data for some ionic crystals which have Frenkel-type defects, Hainovsky and Maier have shown that the correction term due to the defect–defect interaction is proportional to the cube root of concentration [8].

The lowering of the defect's formation energy naturally causes a more rapid increase of defects, which is related to various anomalies in the ionic crystals. Such anomalies can be identified by a rapid increase of the volume, the specific heat, and the ionic conductivity, and a rapid decrease in the elastic constant, etc.

Hereafter we will consider the concentration fluctuation of defects on the basis of statistical thermodynamics. Let $\alpha'(=\ \alpha'_1, \alpha'_2, \alpha'_3, \ldots)$ be the thermodynamic variables of a partial system I, which deviates from a large system under a thermal equilibrium denoted by II, in which variables are expressed by their thermal equilibrium $\alpha^*(=\alpha^*_1, \alpha^*_2, \alpha^*_3, \ldots)$. The probability $P(\alpha')$ indicating the variables α' is given by

$$P(\alpha') = C \exp\{-W_{\min}(\alpha^*, \alpha')/k_B T^*\}, \tag{2}$$

where C is a normalization constant. $W_{\min}(\alpha^*, \alpha')$ is the minimum free energy deviating from that of the thermal equilibrium state α^*.

In the case that an ionic crystal includes Frenkel-type defects, the system is physically equivalent to N_1 defect pairs as solute being dissolved into N_0 ionic pairs of solvent crystal. Thus we can apply the fluctuation theory of a solute in an aqueous solution [9]. The quantity $W_{\min}(\alpha^*, \alpha')$ in such a solution can be written as follows:

$$W_{\min}(\alpha^*, \alpha') = -(\Delta p \Delta V - \Delta T \Delta S - \Delta\mu_1 \Delta N_1)/2, \tag{3}$$

where μ_1 means the chemical potential of a pair of defects in the ionic crystal which is composed of the total number of ion pairs, $N(= N_0 + N_1)$, and ΔX means the fluctuation of X. If equation (3) is expressed in terms of Δp and ΔN_1 under the condition $\Delta T = 0$, we have

$$W_{\min}(\alpha^*, \alpha') = (1/2)\{-(\partial V/\partial p)_{T,N}(\Delta p)^2 + (\partial\mu_1/\partial N_1)_{T,p}(\Delta N_1)^2\}. \tag{4}$$

Therefore the ensemble average of (ΔN_1^2) is given by

$$(\Delta N_1^2)_{\rm av} = k_B T^*/(\partial\mu_1/\partial N_1). \tag{5}$$

On the other hand, the Gibbs free energy with N_1 defect pairs is written as follows:

$$G = (E^*_{\rm perfect} - T^* S^*_{\rm perfect}) + N_1 E_v - k_B T^* \ln\{N!/N_0!N_1!\}. \tag{6}$$

The first round brackets on the right-hand side of this equation indicate the Gibbs free energy of a perfect crystal. The summation of the second and third terms is equal to the Gibbs free energy, which is necessary for the defect formation.

Differentiating G from N_1 we have

$$\mu_1 = (\partial G/\partial N_1)_{p,T} \sim E_v + k_B T^* \ln N_1^*. \tag{7}$$

Here the differentiation for the last term of equation (1) is neglected. Then we have

$$(\partial\mu_1/\partial N_1) = k_B T^*/N_1^*. \tag{8}$$

Putting this relation into (5), we have

$$(\Delta N_1^2)_{\rm av} = N_1^*. \tag{9}$$

Taking the last term in equation (1) into account for the differentiation of E_v, then the obtained value becomes larger than N_1^*, to some extent.

Let us assume a Gaussian function for the probability distribution function for the number of defects, N_1, under the condition that its root-mean-square deviation from N_1^* is equal to $(N_1^*)^{1/2}$ as described in equation (9), then its explicit form is written as follows:

$$P(\Delta N_1) = (1/2\pi N_1^*)^{1/2} \exp\{-(\Delta N_1)^2/2N_1^*\}, \quad (\Delta N_1) = (N_1 - N_1^*). \tag{10}$$

This distribution function suggests that it is easy to get to a large amount of fluctuation of defects being equal to $\pm(N_1^*/2)$. Therefore it is not unreasonable to consider that, locally, the system has parts with a large amount of defects in comparison with its equilibrium value and to form a cluster in which ions are not always to keep the normal solid behavior and then behave like in the liquid state. In the vicinity of the melting point, therefore, it may be possible to have such local clusters moving to and fro in space and time. This situation is certainly equivalent to the occurrence of the heterophase proposed by Frenkel.

We denote this sort of local cluster as the B′-state and all the other remaining parts keeping the condition of the ordinal ionic crystal as the A-state. However, it is emphasized that all these clusters of the B′-state can be created and annihilated dynamically in time and space, keeping only the thermal equilibrium for A $\rightleftarrows$ B′ and appearing macroscopically as one phase; otherwise the system contradicts the Gibbs phase rule. Hereafter we will call this sort of cluster a 'quasi-liquid', in short the 'L'-state. It is interesting to investigate whether its physical properties are similar to those of bulk liquid or not. And there occur various premelting phenomena in the physical properties.

From a different point of view, the appearance of such clusters in the vicinity of the melting point has recently been recognized as the Lindemann instability by using computer simulation [10]. With increasing temperature, therefore, a lattice composed of a mixture of states A and B′ approaches the catastrophe of instability and there occurs a phase transition to the liquid state B. These changes are shown below.

$$\text{(ordinal crystal, A)} \xrightarrow{\text{transition 1}} \text{(mixture of A and B}') \xrightarrow{\text{transition 2}} \text{(liquid phase}B).$$

The transition 1 is a kind of higher-order one like the order–disorder transition. Since the mixture of A and B′ is thermodynamically equal to one phase, this means that some of the physical properties of the cluster B′ itself cannot be distinguished macroscopically. However, it may be possible to define the chemical potential in the cluster $\mu_{B'}$, because it can be determined by each ion pair. We denote the chemical potential of the A-state as μ_A. The transition 2 is, of course, equal to the usual melting.

3. Reconstruction of Frenkel theory

In this section, we will reconstruct the Frenkel theory [6] in a slightly different way and extend it so as to be able to use recent experimental data. Let us consider an ionic crystal with the premelting phenomena, in the vicinity of its melting point. Here we assume that the numbers of positive and negative ions are both equal to N and the number densities of the

liquid state B and of B′-clusters are almost the same, being n_0 ($= N/V_M$; V_M is the molar volume), and in addition we will take $\mu_{B'} \sim \mu_B$ as an approximation. In order to minimize the surface energy, the most ideal shape of a B′-cluster composed of s-pairs is close to a sphere; then we have

$$s = n_0(4\pi r^3/3). \tag{11}$$

The surface area of this sphere is, then, given by $4\pi(3s/4\pi n_0)^{2/3}$, and the corresponding surface free energy, α, is equal to $4\pi\sigma(3s/4\pi n_0)^{2/3}$, where σ is the surface tension per unit area. Therefore, the total chemical potential of this cluster is given by $(s\mu_B + \alpha s^{2/3})$. Let the number of ion pairs belonging to the A-phase be N_A and let the total number of s-pair clusters be equal to g_s; then the total Gibbs free energy of the system, G_{total}, is described as follows:

$$G_{total} = N_A\mu_A + \sum_{s=s0} g_s(s\mu_B + \alpha s^{2/3}) + S_{mix}(g_s, T). \tag{12}$$

In this equation s_0 means the lowest number of ion pairs. $S_{mix}(g_s, T)$ means the mixing entropy and its simplified expression is

$$S_{mix}(g_s, T) = k_BT\left[N_A \ln\left\{N_A \Big/ \left(N_A + \sum g_s\right)\right\} + \sum_s g_s \ln\left\{g_s \Big/ \left(N_A + \sum g_s\right)\right\}\right]. \tag{13}$$

Since the total number of ions is kept constant, we have

$$N_A + \sum_s sg_s = N \tag{14a}$$

or

$$\psi = N - \left(N_A + \sum_s sg_s\right) = 0. \tag{14b}$$

By using the method of Lagrange multipliers, the condition of minimizing the G_{total} value is given by the following relation:

$$\{(\partial G_{total}/\partial N_A) + (\lambda\partial\psi/\partial N_A)\}\,dN_A + \{(\partial G_{total}/\partial g_s) + (\lambda\partial\psi/\partial g_s)\}\,dg_s = 0. \tag{15}$$

Taking $\lambda = -\ln C$, we have

$$\left\{g_s \Big/ \left(N_A + \sum g_s\right)\right\} = C^l \exp[-\beta(s\mu_B + \alpha s^{2/3})] \tag{16}$$

and

$$\left\{N_A \Big/ \left(N_A + \sum g_s\right)\right\} = C\exp[-\beta\mu_A], \tag{17}$$

where $\beta = 1/k_BT$ and l is a constant value which it is not necessary to specify. Combining equations (13), (16) and (17), we have

$$g_s = \left(N_A + \sum g_s\right)\left\{N_A \Big/ \left(N_A + \sum g_s\right)\right\}^l \times \exp[-\beta\{s(\mu_B - \mu_A) + \alpha s^{2/3}\}]. \tag{18}$$

The total fraction of clusters seems to be much smaller in comparison with N; that is, $\sum g_s \ll N_A \sim N$. Therefore, we have

$$g_s \simeq \left(N_A + \sum g_s\right)\left\{1 - \left(l\sum g_s/N_A\right)\right\} \times \exp[-\beta\{s(\mu_B - \mu_A) + \alpha s^{2/3}\}] \simeq N\exp[-\beta\{s(\mu_B - \mu_A) + \alpha s^{2/3}\}]. \tag{19}$$

At the temperature T just below the melting point T_m, the chemical potentials μ_A and μ_B are thermodynamically given by the following relation:

$$\mu_B - \mu_A = \{(\partial\mu_B/\partial T)_{T_m} - (\partial\mu_A/\partial T)_{T_m}\}(T - T_m) = \{(s_A)_{T_m} - (s_B)_{T_m}\}(T - T_m), \tag{20}$$

where $(s_A)_{T_m}$ and $(s_B)_{T_m}$ are equal to the entropies of the states A and B. Therefore, by using the latent heat of fusion L_m, we have

$$\{(s_A)_{T_m} - (s_B)_{T_m}\} = -(L_m/NT_m) \tag{21}$$

and

$$\mu_B - \mu_A = -(L_m/NT_m)(T - T_m). \tag{22}$$

Putting (22) into (19), we have

$$g_s = N\exp[-\beta\{s(L_m/NT_m)(T_m - T) + \alpha s^{2/3}\}]. \tag{23}$$

Combining (12), (13), (16) and (17), we have

$$G_{total} = Nk_BT\ln C = N\mu_A - Nk_BT\ln\left\{N_A \Big/ \left(N_A + \sum g_s\right)\right\} \sim N\mu_A - Nk_BT\left(\sum g_s/N_A\right). \tag{24}$$

Insertion of (23) into (24) gives the following relation:

$$G_{total} = N\mu_A - Nk_BT\sum_{s=s0}\exp[-\beta\{s(L_m/NT_m)(T_m - T) + \alpha s^{2/3}\}]. \tag{25}$$

If the number of ion pairs s is regarded as continuous with its lowest value s_0, then the above equation is described by an integration form as follows:

$$G_{total} = N\mu_A - Nk_BT\int_{s0}^{\infty}\exp[-\beta\{s(L_m/NT_m)(T_m - T) + \alpha s^{2/3}\}]\,ds. \tag{26}$$

It is emphasized that the Gibbs free energy of the present system is lowered by the mixture of (A-state + B′-state) rather than the homogenized A-state. In other words, the appearance of the clusters indicated by the B′-state seems plausible from the viewpoint of thermodynamic conditions.

By using the Gibbs–Helmholtz equation, the enthalpy change, ΔH, corresponding to the second term on the right-hand side of equation (26) is equal to

$$\Delta H = L_m\int_{s0}^{\infty} s\exp[-\beta\{s(L_m/NT_m)(T_m - T) + \alpha s^{2/3}\}]\,ds. \tag{27}$$

4. Anomalous specific heats of ionic crystals in the neighborhood of their melting points

Hainovsky and Maier [8] were successful in explaining the thermodynamic anomalies in some Frenkel-type defected ionic crystals. In particular, they obtained the defects' fractions by analyzing the temperature dependences of the specific heats.

In contrast, we will derive the value of the anomalous specific heat at the melting point by using (27) and investigate how its value varies with $(T_m - T)$. Applying the Maxwell

relation to (27), we have the specific heat of the system (mixture of A and B′) at the melting point, $C_p(T_m)$, as follows:

$$C_p(T_m) = C_p^A(T_m) + (L_m^2/Nk_BT_m^2)\int_{s0}^{\infty} s^2 \exp[-\beta(\alpha s^{2/3})]\,ds, \tag{28}$$

where $C_p^A(T_m)$ is the normal specific heat in the A-state only case at $T = T_m$. The normal specific heat of the A-state, $C_p^A(T)$, where only some defects are distributed randomly, may be expressed by a linear temperature dependence, as will be discussed below. The last term of (28) was already obtained by Frenkel [6].

Our task is to extend equation (28) so as to be able to compare with the observed specific heats in order to obtain the cluster sizes of the B′-state. Carrying out the partial integration for the last term of equation (28), we obtain

$$C_p(T_m) = C_p^A(T_m) + (3/2)(L_m^2/Nk_BT_m^2) \times \left[(1/\beta\alpha)s_0^{7/3}\exp\{-\beta\alpha s_0^{2/3}\} + (17/6\beta\alpha)\int_{s0}^{\infty} s^{4/3}\exp\{-\beta\alpha s^{2/3}\}\,ds\right]. \tag{29}$$

If we assume that the distribution of the cluster sizes is rather sharp around the value of $\hat{s}$, which number is also close to the lowest one s_0, then we have the following form instead of (29):

$$C_p(T_m) \sim C_p^A(T_m) + (3/2)(L_m^2/Nk_BT_m^2) \times [(1/\beta\alpha)\hat{s}^{7/3}\exp\{-\beta\alpha\hat{s}^{2/3}\} + (17/6\beta\alpha)\hat{s}^{4/3} \times \exp\{-\beta\alpha\hat{s}^{2/3}\}] \sim C_p^A(T_m) + (3/2)(L_m^2/Nk_BT_m^2) \times [(1/\beta\alpha)\hat{s}^{7/3}\exp\{-\beta\alpha\hat{s}^{2/3}\}]. \tag{30}$$

By using (30), the specific heat at the temperature T in the vicinity of the melting point, $C_p(T)$, is expressed as follows:

$$C_p(T) \sim C_p^A(T_m) + \Delta C_p(T_m)\exp[L_m\hat{s}/Nk_BT_m] \times \exp[-L_m\hat{s}/Nk_BT], \tag{31}$$

where

$$\Delta C_p(T_m) = (3/2)(L_m^2/Nk_BT_m^2)[(1/\beta\alpha)\hat{s}^{7/3}\exp\{-\beta\alpha\hat{s}^{2/3}\}]. \tag{32}$$

The normal specific heat of state A at temperature T is usually determined by the defects' formation energy and the unharmonic term in the lattice vibration in addition to the classical Dulong–Petit's value. The former two terms are linearly but gently proportional to the temperature as known from various experiments under the condition of no defect–defect interaction.

The anomalous specific heat in the vicinity of the melting point is caused by the second term on the right-hand side of equation (31). In a later section, we will obtain the magnitude of clusters denoted by $\hat{s}$, by using the observed specific heats and all other available data of solid AgBr and NaCl.

5. Determination of ion pairs' numbers of averaged clusters and their total fractions

In this section, we will briefly discuss the total fraction of 'L' or 'quasi-liquid' clusters. We also assume that there exist clusters of which the number of ion pairs is only $\hat{s}$ as the mean value for simplicity. Let us denote the fraction of ionic pairs belonging to the 'L' clusters as g. This fraction can be written as follows:

$$g = \hat{s}g_s/N = \hat{s}\exp[-\beta\{s(\mu_B - \mu_A) + \alpha s^{2/3}\}]. \tag{33}$$

At a temperature $T \sim T_m$, we have

$$g(T) = \hat{s}\exp[-\beta\{\hat{s}(L_m/NT_m)(T_m - T) + \alpha\hat{s}^{2/3}\}] \tag{34}$$

and at a temperature a $T = T_m$,

$$g(T_m) = \hat{s}\exp[-\beta(\alpha\hat{s}^{2/3})]. \tag{35}$$

Hereafter, we will determine some quantitative magnitudes of the 'L' clusters of AgBr and NaCl as case studies.

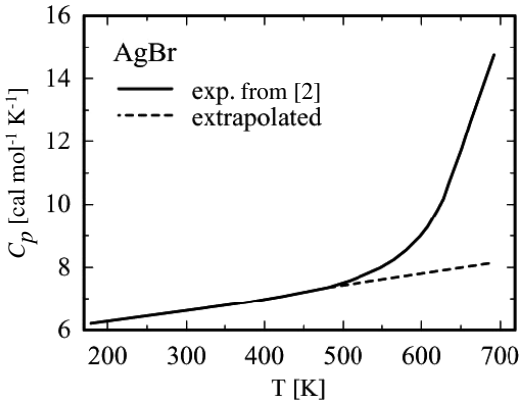

Figure 1. Temperature dependence of C_p after reference [2].

5.1. Case study for AgBr which has Frenkel-type defects

Fortunately, the experimental study on the specific heat of solid AgBr has been carried out up to the melting point by Jost and Kubaschewski [2].

According to their experimental results, we know that $C_p(T_m) = 14.85$ cal mol^{-1} K^{-1}, $C_p^A(T_m) = 8.15$ cal mol^{-1} K^{-1}, which can be obtained from a linear extrapolation to the melting point. Then, the anomalous specific heat is equal to $\Delta C_p = 6.7$ cal mol^{-1} K^{-1}, as shown in figure 1. Other data necessary for the estimation of $\hat{s}$ are $T_m = 703$ K, $L_m = 2199.1$ cal mol^{-1} and $\beta\alpha \sim 1/7$, which is inferred from the surface tension of molten NaCl. Inserting these quantities into (30), we have

$$\hat{s} \sim 1553.$$

Putting this value into (35), we also have

$$g(T_m) \sim 0.74 \times 10^{-5}.$$

5.2. Case study for NaCl which has Schottky-type defects

The known experimental data are $T_m = 1073$ K, $L_m = 7220$ cal mol^{-1}, $\sigma = 116$ CGS unit [11], and $\alpha = 1.38 \times 10^{-13}$

Table 1. Temperature dependence of δ_L of the system.

NaCl		AgBr	
T (K)	δ_L	T (K)	δ_L
1148	1.0535	883	0.5706
1074	0.2135	703	0.2536
973	0.1782	604	0.1877
300	0.0882	300	0.1268

CGS unit; therefore we have $\beta\alpha \sim 1/6$. Since there is at present no satisfactory information on the specific heat up to the melting point, we will assume acceptable quantities, such as $C_p(T_m) = 15$ cal mol^{-1} K^{-1}, $C_p^A(T_m) = 7$ cal mol^{-1} K^{-1}, and $\Delta C_p = 8$ cal mol^{-1} K^{-1}; putting these values into (30), then we have immediately

$$\hat{s} \sim 856.$$

Putting this value into (35), we have

$$g(T_m) = 1.00 \times 10^{-3}.$$

This fraction is somewhat bigger than the case of AgBr. However, its value may be a plausible fraction.

Under these populations of 'L' clusters, it is not easy to keep the inverse lattice periodicity for the ion's one-body distribution and one can expect a catastrophe in the crystal array i.e. more distorted ion distrubution. In fact, Jin *et al* have shown that the Lindemann instability of Lennard-Jones particles in a face-centered cubic box prevails over a wide region of liquid-like clusters consisting of about 300 particles, the size of which was found to be stable [10].

According to Hainovsky and Maier [7], the defect fraction in Frenkel-type defected crystals like AgCl and AgBr approaches to the order of 1.00×10^{-4}. Therefore the fraction of defects in the clusters in such crystals, f', must be $f' \geqslant 1.00 \times 10^{-4}$. If the fraction f' is in the range 10^{-2}–10^{-3}, it may be easy for an instability of the periodicity to occur to begin the melting.

6. Molecular dynamics simulation

So far, we have discussed the premelting features on the basis of the re-examined Frenkel theory. Meanwhile, there have been number of reports on the melting of crystals from both statistical thermodynamics [12] and the dynamics of atoms or ions [13], since Lindemann proposed the instability of crystals [14].

One of the most effective ways to confirm the above results and to examine the ionic configuration detail is molecular dynamics (MD) simulation. We have performed MD simulations in the NaCl and AgBr systems. The detailed simulation procedure is essentially the same as used before [15]. We briefly describe it, as follows. The Tosi–Fumi-type pair potentials are used in the MD simulation for NaCl, which are expressed as [16]

$$V_{ij}(r) = B_{ij}\exp(-a_{ij}r) + z_i z_j e^2/r - C_{ij}/r^6, \qquad (36)$$

Table 2. Average of δ_L for 'L' and 'non-L' ions.

NaCl at 1074 K	δ_L	AgBr at 703 K	δ_L
'L' Na ions	0.26	'L' Ag ions	0.32
'L' Cl ions	0.27	'L' Br ions	0.26
'non L' ions	0.20	'non L' ions	0.22

where the first term represents the short-range repulsion between ions; the second term stands for the Coulomb interactions with the charge of ions, z_i and z_j; and the third term represents the van der Waals interactions.

For AgBr, we adopt the Rahman, Vashishta and Parrinello (RVP) [17] type potentials, because they are often used for noble-metal halides. The RVP-type potentials for i and j ions are written as

$$V_{ij}(r) = H_{ij}/r^{nij} + z_i z_j e^2/r - P_{ij}/r^4 - C_{ij}/r^6, \qquad (37)$$

where the first term stands for the repulsion between ions; the second is the Coulomb interaction; the third term is charge–dipole interactions; and the fourth term is the van der Waals contributions. The adopted parameter values are taken from the literature [16, 18]. The MD calculations are carried out for NaCl and AgBr using 8000 atoms (4000 cations and 4000 anions) placed in a cubic cell, which may include the expected whole 'L' cluster. The number densities used are taken from experiments [19]. The periodic boundary condition is used. The Coulomb interaction is calculated by the Ewald method. At first the cell is equilibrated at a constant temperature; then the calculation of the structure is carried out on the condition that the number of the particles, the volume of the cell and the total energy of the system (NVE) are constant.

In order to examine the detail of premelting phenomena in ionic crystals, we evaluated the Lindemann instability criterion, which is expressed by Lindemann ratio δ_L, which is obtained by the root-mean-square displacement of the particle in question at $\mathbf{r}_i(t)$ from its original lattice site $\mathbf{R}_i(0)$, $\langle\Delta\mathbf{r}^2\rangle^{1/2} = \langle(\mathbf{r}_i(t) - \mathbf{R}_i(0))^2\rangle^{1/2}$, divided by the average nearest-neighbor distance $\langle\mathbf{r}_{kl}\rangle$ [10]. The temperature dependence of the system average δ_L for NaCl and AgBr is listed in table 1.

The calculations of δ_L are performed at temperatures corresponding to the molten phase, melting point, 100 K below the melting point, and solid phase at room temperature, respectively. The obtained δ_L values show the similar temperature dependence as in Lennard-Jones (LJ) crystals [10], which means that δ_L is also effective as a premelting feature in ionic crystals. We adopt the critical Lindemann ratio, $\delta_c = 0.24$, in order to distinguish 'Lindemann particles', which we have referred to as 'quasi-liquid' or 'L' particles in previous sections, from the 'solid-like' particles or 'non-L' particles. The estimated numbers of 'L' particles at the melting point of NaCl and AgBr crystals are 806 Na and 719 Cl, and 2256 Ag and 958 Br, respectively. These evaluations are comparable with the ion numbers estimated by the theory, 1712 and 3150 for total 'L' ions in NaCl and AgBr, respectively. The average of δ_L for 'L' and 'non-L' ions in NaCl and AgBr at 1074 K and 703 K, respectively, are listed in table 2.

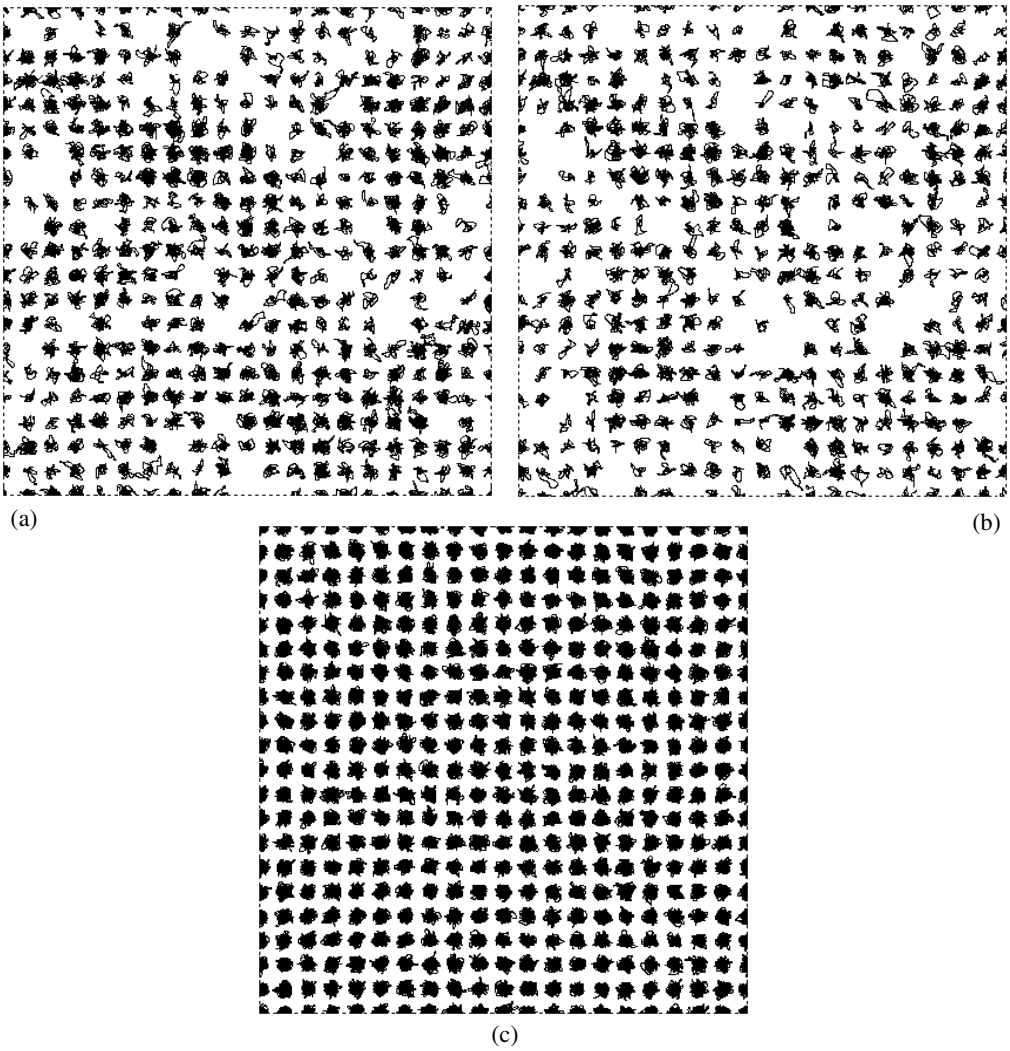

Figure 2. (a) Trajectories of Na Lindemann particles in NaCl crystal at 1074 K. (b) Trajectories of Cl Lindemann particles in NaCl crystal at 1074 K. (c) Trajectories of non-Lindemann particles in NaCl crystal at 1074 K.

The obtained average δ_L for 'L' ions of Na, Cl and Br are about 0.26; on the other hand, the average δ_L for 'L' ions of Ag is 0.32, which indicates a mobile feature of 'L' ions of Ag. The value 0.22 was used by Jin *et al* [10] as δ_c for Lennard-Jones (LJ) crystals;, however, it seems to yield an overestimation of the number of 'L' particles in NaCl and AgBr, 3067 and 4392 of the total 'L' ions, respectively. These results may be caused by the fact that the interactions between particles in ionic crystals are different from those in LJ particles. The typical examples of trajectories of 'L'-type Na and Cl projected on x–y planes are shown in figures 2(a) and (b), respectively; they are obviously different from those of 'non-L' ions in figure 2(c). The cluster-like structures are clearly seen in figures 2(a) and (b). Regarding AgBr, as is seen in figure 3(b), the Br ions form cluster-like structures, which resemble the 'L' ions in NaCl. The trajectories of Ag ions in figure 3(a), however, show a more spread distribution, and a cluster-like feature is also observed. According to the experimental study on the structure of AgBr, Frenkel-type disorder of Ag in the Br sublattice occurs before melting. However, the transition to the superionic phase in AgBr at high temperature, which is observed in some noble-metal halides, e.g. AgI, seems to be prevented by melting [20, 21]. The present results by MD simulation of trajectories of Ag and unequal 'L' particle numbers of Ag and Br correspond to these experimental facts.

The partial pair distribution functions, $g_{ij}(r)$, are calculated to examine the ionic configuration details; they are obtained from an average of 400–600 MD time steps. The $g_{ij}(r)$ obtained for NaCl in the premelting region for 'L' and 'non-L' ions are shown in figures 4(a) and (b), respectively, with those of the molten and solid phase for comparison. The obtained $g_{ij}(r)$ of 'non-L' ions of NaCl have similar features to those of the solid phase. In the $g_{ij}(r)$ of 'L' ions in NaCl, the peaks and troughs (except the first peaks) become flatter than those of 'non-L' ions, though their features are still those of the solid phase. The $g_{ij}(r)$ of 'non-L' ions of AgBr are shown in figure 5(b); they also resembles those of the solid phase. On the other hand, the $g_{ij}(r)$ of 'L' ions, especially $g_{\mathrm{AgAg}}(r)$, have more liquid-like features in figure 5(a), though the peaks and small shoulders that originate in the solid structure are still observed.

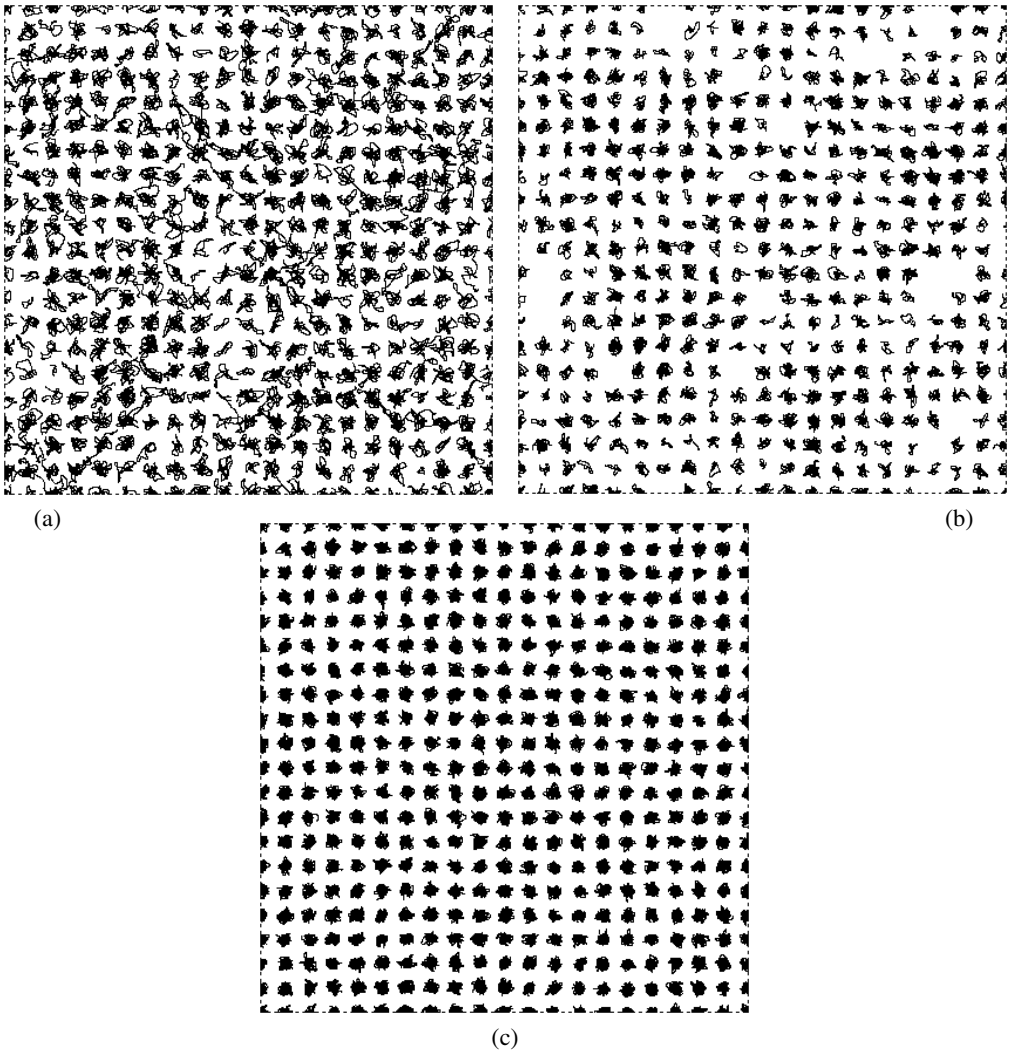

Figure 3. (a) Trajectories of Ag Lindemann particles in AgBr crystal at 703 K. (b) Trajectories of Br Lindemann particles in AgBr crystal at 703 K. (c) Trajectories of non-Lindemann particles in AgBr crystal at 703 K.

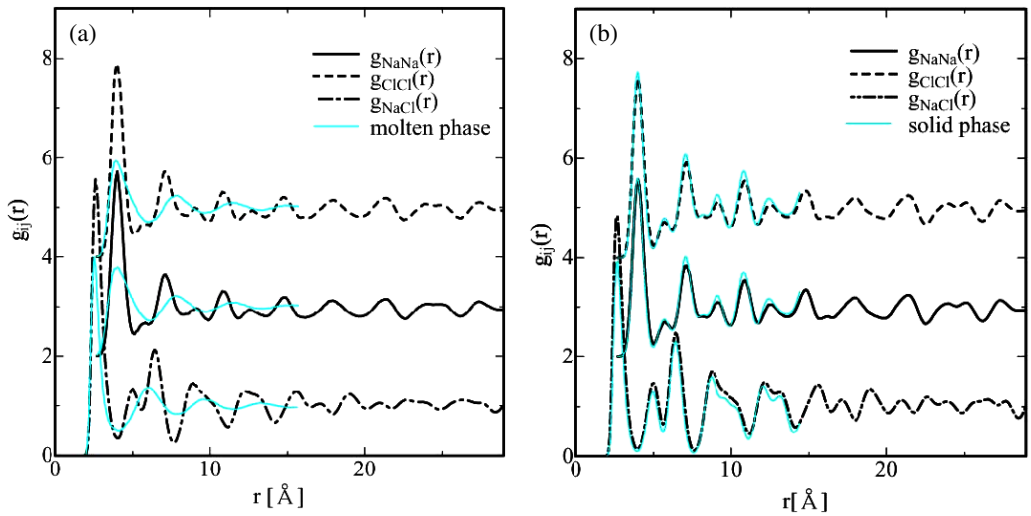

Figure 4. (a) $g_{ij}(r)$ of Lindemann particles in NaCl at 1074 K together with those of the molten phase (thin solid line). (b) $g_{ij}(r)$ of non-Lindemann particles in NaCl at 1074 K together with those of the solid phase, 100 K below the melting point (thin solid line).

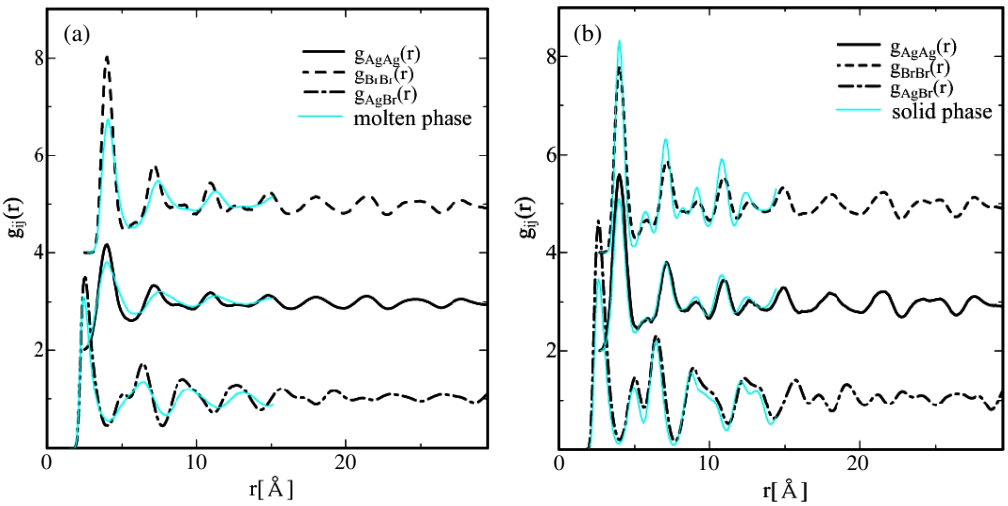

Figure 5. (a) $g_{ij}(r)$ of Lindemann particles in AgBr at 703 K together with those of the molten phase (thin solid line). (b) $g_{ij}(r)$ of non-Lindemann particles in AgBr at 703K together with those of the solid phase, 100 K below the melting point (thin solid line).

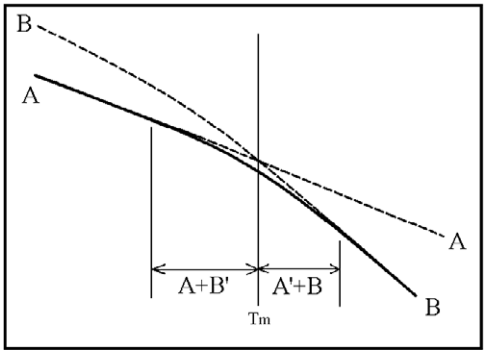

Figure 6. Macroscopic $G(= N\mu)$–T curves with the coexistence of A′ and B′ around T_m.

7. Discussion

In section 6, we obtained the cluster distribution of 'L' particles in NaCl and AgBr, and their numbers are comparable with the value estimated by the theory. However, the estimated ratio of ion pairs associated with the clusters of 'L' particles to the total number of ion pairs in NaCl g (at T_m) is 1.00×10^{-3}, which could not be reproduced by the present MD simulation. Using the postulate that the distribution of clusters is given by a binomial or corresponding Gaussian probability distribution function, the distance between any two clusters can approach about three times the spherical diameter, although the most possible distance is approximately equal to ten times the spherical diameter with probabilities about 0.015 and 0.175, respectively. This fact may suggest that larger-scale MD simulations are required to estimate $g(T)$ and the inter-cluster distance.

The 'L' cluster obtained in the MD simulation seems to separate into smaller parts. This may be explained as follows. The occurrence of 'L' clusters causes a lowering of Gibbs free energy, as shown in (25) or (26), which is schematically shown in figure 6. Its lowering of energy is approximately equal to 0.005 cal mol^{-1}. This magnitude may indicate that the melting point itself is scarcely varied by such an appearance of 'L' clusters, and the cluster distribution in the cell rearranges to lower the Gibbs free energy.

Acknowledgments

One of the authors (SM) expresses his thanks for the financial support by Nippon Sheet Glass Foundation for Materials Science and Engineering. He is also grateful to the Ministry of Education, Science and Culture for financial support by a Grant-in-Aid for Science Research. Parts of the simulation results in this research were obtained using supercomputing resources at the Information Synergy Center, Tohoku University.

References

[1] See for examples Green P F 2005 *Kinetics, Transport, and Structure in Hard and Soft Materials* (London: Taylor and Francis)
Chiang Y-M, Birnie D P and Kingery W D 1997 *Physical Ceramics: Principles for Ceramic Science and Engineering* (New York: Wiley)
[2] Jost W and Kubaschewski P 1968 *Z. Phys. Chem.* **60** 69
Christy R W and Lawson A W 1951 *J. Chem. Phys.* **19** 517
Kanzaki H 1951 *Phys. Rev.* **81** 884
[3] Lawson B R 1963 *Acta Crystallogr.* **16** 1163
[4] Yamamoto S, Ohno I and Anderson O L 1987 *Phys. Chem. Solids* **48** 143
Hughes W C and Cain L S 1996 *Phys. Rev.* B **53** 5174
Cain L S and Hu G 2001 *Phys. Rev.* B **64** 104104
[5] Ubbelohde A R 1965 *Melting and Crystal Structure* (Oxford: Clarendon)
[6] Frenkel J 1939 *J. Chem. Phys.* **7** 200
Frenkel J 1939 *J. Chem. Phys.* **7** 538
[7] Kurosawa T 1957 *J. Phys. Soc. Japan* **12** 338
[8] Hainovsky N and Maier J 1995 *Phys. Rev.* B **51** 15789

[9] Kubo R (ed) 1978 *Exercises in Thermodynamics and Statistical Mechanics* (Tokyo: Shokabō) (in Japanese)
[10] Jin Z H, Gumbsch P, Lu K and Ma E 2001 *Phys. Rev. Lett.* **87** 55703
[11] March N H and Tosi M P 1976 *Atomic Dynamics in Liquids* (London: MacMillan)
[12] Kirkwood J G and Monroe E 1940 *J. Chem. Phys.* **8** 623
Brout R 1965 *Phase Transitions* (New York: Benjamin)
[13] Born M 1939 *J. Chem. Phys.* **7** 591
Born M and Huang H 1988 *Dynamical Theory of Crystal Lattices* (Oxford: Clarendon)
[14] Lindemann F 1910 *Z. Phys.* **11** 609
[15] Matsunaga S, Koishi T and Tamaki S 2007 *Mater. Sci. Eng.* A **449** 693
Matsunaga S, Saito M, Koishi T and Tamaki S 2007 *Mol. Simul.* **33** 153
Matsunaga S 2005 *Solid State Ion.* **176** 1929
Matsunaga S and Madden P A 2003 *J. Phys.: Condens. Matter* **16** 181
[16] Sangster M J L and Dixon M 1976 *Adv. Phys.* **25** 247
[17] Parrinello M, Rahman A and Vashishta P 1983 *Phys. Rev. Lett.* **50** 1073
[18] Tasseven C, Trullàs J, Alcaraz O, Silbert M and Giro A 1997 *J. Chem. Phys.* **106** 7286
[19] Enck F D and Dommel J G 1964 *J. Appl. Phys.* **16** 44
Lawn B R 1963 *Acta Crystallogr.* **16** 1163
[20] Andreoni W and Tosi M P 1983 *Solid State Ion.* **11** 49
[21] Nield V M, Keen D A, Hayes W and McGreevy R L 1992 *J. Phys.: Condens. Matter* **4** 6703